

Screening and Simulation Study of Efficacious Antiviral Cannabinoid Compounds as Potential Agents Against SARS-CoV-2

Mahima Devi^a and Vivek Kumar Yadav^{b*}

(a) Department of Bio-informatics, University of Allahabad, Prayagraj, UP 221001, India

(b) Department of Chemistry, University of Allahabad, Prayagraj, UP 221001, India

Abstract

The proliferation of severe acute respiratory syndrome corona-virus 2 (SARS-CoV-2) and the persistent corona-virus disease 2019 (COVID-19) pandemic emphasize the necessity for novel treatments. Among the diverse pharmacological agents under scrutiny, cannabinoids have garnered attention for their potential antiviral properties. This study utilizes molecular docking and simulation techniques to explore the interaction between cannabinoids drugs and essential SARS-CoV-2 viral proteins, aiming to identify potential therapeutic effects. The results suggest favorable binding energies between certain cannabinoids drugs and viral proteins, especially at the active sites of the spike protein. Our computational findings reveal that the ligands Cannabiscitrin and Cannabisin D exhibit the highest binding affinity (approximately -9.11 and -8.84 kcal/mol, respectively) toward the SARS-CoV-2 receptor, while Alacepril displays the lowest affinity (-6.32 kcal/mol) for the SARS-CoV-2 receptor. The findings suggest a potential inhibitory effect of cannabinoid drugs on both viral entry and replication. Furthermore, simulations demonstrate cannabinoid binding to the CB2 receptor, suggesting potential immunomodulatory roles in SARS-CoV-2 infection. This research underscores the promise of cannabinoids as SARS-CoV-2 therapeutic agents, necessitating further validation and clinical exploration.

Keywords

Docking, antiviral cannabinoid drugs; Sars-CoV-2; Molecular Dynamics.

1 Introduction

The world stood witness to an unprecedented and deadly outbreak of COVID-19, a disease caused by the severe acute respiratory syndrome corona-virus 2 (SARS-CoV-2) [1]. Originating in Wuhan City, Hubei, China, this virulent virus quickly traversed borders and infected populations worldwide [2,3]. COVID-19 is characterized by a spectrum of symptoms, ranging from respiratory distress, fever, and pneumonia to sore throats and lung infections [4,5]. Recognizing the gravity of the situation, WHO declared the COVID-19 outbreak a Public Health Emergency of International Concern on January 30th, 2020 [6]. As of June 22, 2020, the WHO had documented a staggering 8,860,331 confirmed cases and 465,740 deaths worldwide, underscoring the magnitude of the pandemic [7]. Globally, as of 8 November 2023, there have been 772,166,517 (about 45,001,575 in India) confirmed cases of COVID-19, including 6,981,263 (about 533,295 in India) deaths, reported to WHO [8]. Even with the recent availability of vaccines, SARS-CoV-2 continues to spread rapidly [9], emphasizing the necessity for alternative treatments, particularly for populations with limited inclination or access to vaccines. To date, only a limited number of therapies have been identified that can effectively block SARS-CoV-2 replication and viral production [10].

The search for effective antiviral agents against SARS-CoV-2 has become an urgent priority, necessitating the exploration of diverse pharmacological compounds [11]. Cannabinoids, a class of compounds primarily derived from the Cannabis sativa plant, have garnered substantial attention due to their broad pharmacological effects, including anti-inflammatory, immunomodulatory, and potential antiviral properties [12,13]. In cannabinoids, the Cannabinoid type 2 (CB2) ligands, a class of compounds that interact with the CB2 receptors in the endocannabinoid system, have shown promising antiviral activity [14-16]. These ligands exhibit a potential inhibitory impact on viral entry and replication, suggesting a role in impeding the spread of viruses [17-20]. Particularly relevant to the ongoing challenges posed by SARS-CoV-2, simulations have revealed the binding of cannabinoids to the CB2 receptor, indicating their potential immunomodulatory roles in combating viral infections [21-24]. The exploration of CB2 ligands as antiviral agents represents a novel avenue in the quest for effective treatments against viral pathogens [25]. Recent research has suggested that cannabinoids may hold promise as agents capable of mitigating viral infections [26,27]. Despite multiple studies and various unverified claims regarding CBD-containing products, the biological actions of CBD itself remain unclear, and specific targets are largely unknown [28]. While limited, certain studies have reported that particular cannabinoids demonstrate antiviral effects against viruses such as the hepatitis C virus and others [29]. The cannabis plant contains over 550 chemical constituents, with approximately 150 being cannabinoids and more than 400 non-cannabinoids [30]. The primary pharmacologically active compounds include the psychoactive tetrahydrocannabinols (THC), such as Δ^8 -THC and Δ^9 -THC, along with non-psychoactive cannabinoids like cannabitol (CBN), cannabidiol (CBD), and cannabigerol (CBG), among others [31-34].

This paper presents a comprehensive investigation into the potential of certain cannabinoid compounds as antiviral agents against SARS-CoV-2 through a combination of screening and simulation techniques. The favorable binding interactions observed between selected cannabinoids and viral proteins suggest their ability to interfere with critical viral processes. Moreover, the binding of cannabinoids

*Corresponding author Email: vkyadav@allduniv.ac.in

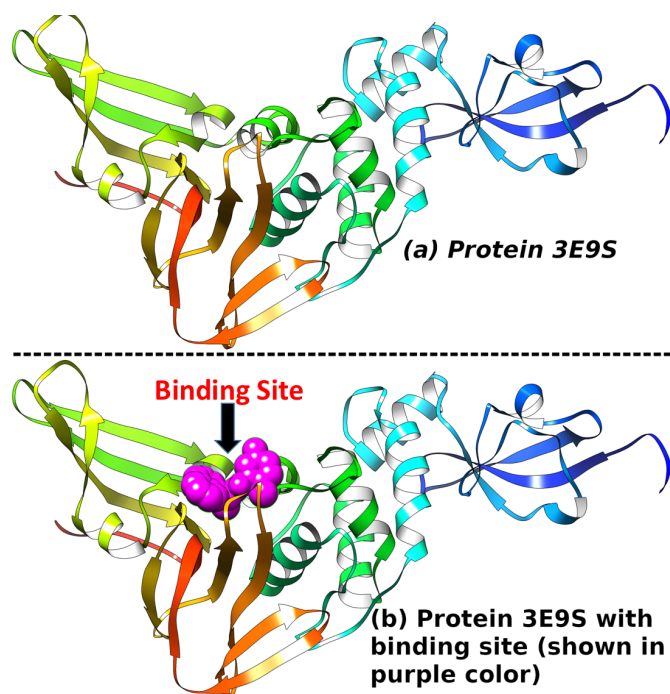


Fig. 1 SARS-CoV-2 protein structure (PDB ID: 3E9S) (a) without and (b) with binding site, respectively.

to the CB2 receptor highlights their potential immunomodulatory properties, which may play a crucial role in regulating the immune response during SARS-CoV-2 infection. Further experimental studies are warranted to validate these findings and explore the clinical implications of cannabinoid-based therapies in combating COVID-19. Finally, we conclude with a succinct summary of our significant findings obtained throughout this study.

2 Methodology

2.1 Preparation of Protein and selection of ligands

The 3D crystal structure of the SARS-CoV-2 receptor binding domain (RBD) of the spike protein complexed with the human ACE2 receptor (PDB ID: 3E9S) and Cannabinoid type-2 receptor (PDB ID: 2YDO), were downloaded from the RCSB Protein Data Bank (PDB) [35]. To get pure protein, all ligands attached are removed using PyMOL software and saved the processed file in PDB format [36]. To avoid the interference of water molecules in the pocket region, we used auto-dock tools [37] that deleted water molecules from 3D structure of nucleoprotein. Then polar hydrogen atoms are added in the protein. Further, the protein structure was prepared for drug docking using AutoDockTools software [37]. Hydrogen atoms were added to the protein, and non-polar hydrogens were merged. The polar hydrogen charges were then assigned using the Gasteiger method. The protein was then saved in the PDBQT format, which is compatible with the AutoDockVina software used for molecular docking simulations. The cannabinoid ligands selected for this study were Cannabis. These compounds were chosen because they have been previously reported to have antiviral properties and are easily accessible for experimental studies [15,16]. The 3D structure of the eight compounds was downloaded in SDF format via the ZINC database [38] and details are reported in Table 1. Choose ligand and then select molecule for auto-dock. Next step is to save as pdbqt file. Now we have the files Cannabinol.pdbqt and Cannabiscitrin.pdbqt. In this way, second step of docking is completed. Fig. 2 shows the prepared view of ligand Alacepril, Myricetin, Cannabidiol Acid, Cannabigerol, Cannabigerolic Acid, and Cannabisin D are also prepared using the same procedure.

2.2 Molecular docking methodology

Molecular docking were performed using the Auto-Dock Vina software [39]. The protein structure of the SARS-CoV-2 RBD and Cannabinoid type-2 receptor were used as the target proteins, while the cannabinoid drugs were used as the ligands. For 3E9S, the grid box was defined to encompass the entire RBD protein with a size of 60 x 60 x 60 Å³, a grid spacing of 0.5 Å, and x, y, z center grid box (-31.02, 21.89, 30.09). For 2YDO the grid box was defined to encompass the entire RBD protein with a size of 60 x 60 x 60 Å³, a grid spacing of 0.572 Å³ and x, y, z center grid box (-35.02, 6.109, -21.757). The exhaustiveness parameter was set to 50, which is the maximum number of binding modes to be searched. The binding energies of the docked complexes were calculated and ranked according to their binding affinity, expressed in kcal/mol. The lowest binding energy (more negative energy) conformation was considered the most energetically favorable and was selected for further analysis. The interactions between the cannabinoids and the amino acid residues

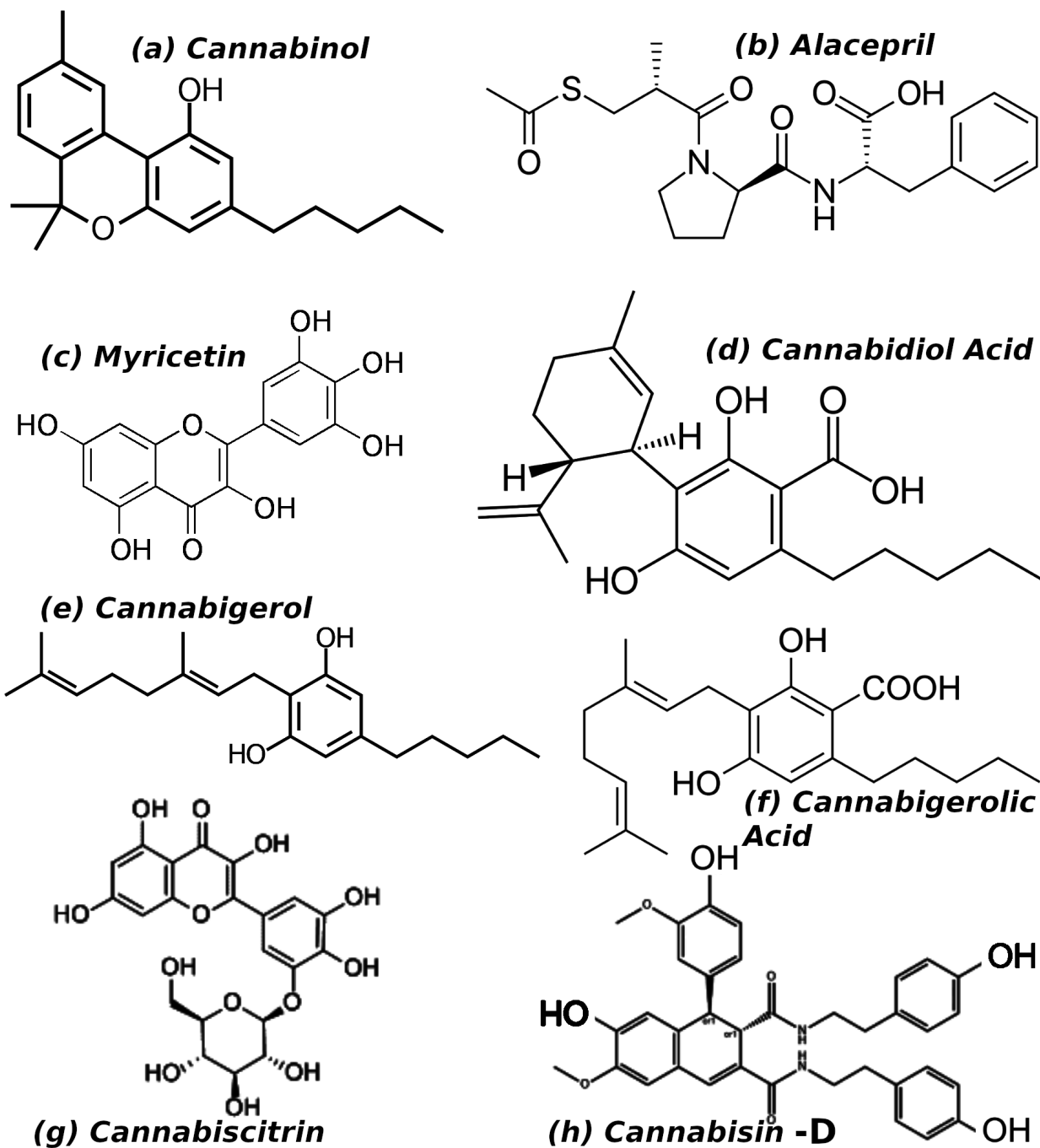


Fig. 2 2D structure of the eight Cannabinoid ligands

S.No.	Compound	ZINC ID	Molecular formula	Mole. Wt.	HBD	HBA	Antiviral activity (Study)
1	Cannabinol	1530833	C21H26O2	310.437	1	2	Yes (In vitro)
2	Alacepril	3775143	C20H26N2O5S	406.504	1	6	Yes (In vitro)
3	Myricetin	3874317	C15H10O8	318.237	4	8	Yes (In vitro)
4	Cannabidiol Acid	4098864	C22H30O4	358.478	2	4	Yes (In vitro)
5	Cannabigerol	4217650	C21H32O2	316.485	2	2	Yes (In vitro)
6	Cannabigerolic Acid	8773249	C22H32O4	360.494	2	4	Yes (In vitro)
7	Cannabicitrin	14436714	C21H20O13	480.378			Yes (In vitro)
8	Cannabisin D	44307185	C36H36NO8	624.69	6	8	Yes (In vitro)

Table 1 The molecular formula, molecular weight, hydrogen bond donor, hydrogen bond acceptor, rotatable bonds, and ZINC ID of eight compounds.

of the SARS-CoV-2 RBD and cannabinoid type-2 were analyzed, and the binding modes were compared to identify the most favorable binding mode. The binding affinity of each ligand was calculated and compared.

2.3 Molecular dynamics simulation methodology

After the molecular docking, the SARS-CoV-2 RBD and cannabinoid type-2 complexed with the best docked ligands was subjected to molecular dynamics (MD) simulation using the GROMACS software^[40]. The system was first energy minimized using the steepest descent algorithm with a maximum of 5000 steps or until a convergence threshold of 1000 kJ/mol was reached. The MD simulation was carried out using the CHARMM36 force field^[41] with the Particle Mesh Ewald (PME) method for long-range electrostatic interactions. The time step was set to 2 fs, and the temperature and pressure were maintained at 300 K and 1 bar, respectively, using the Nose-Hoover thermostat and the Parrinello-Rahman barostat^[42-44]. The system was simulated for 50 ns, and the trajectories were saved every 10 ps for analysis. The stability and convergence of the MD simulations were assessed by monitoring the root mean square deviation (RMSD) of the protein-ligand complex and the root mean square fluctuation (RMSF) of the protein backbone residues. The equations are as follows:

$$RMSD_x = \sqrt{\frac{1}{N} \sum_{i=1}^N (r_i(t_x) - r_i(t_{ref}))^2}$$

$$RMSF_i = \sqrt{\frac{1}{T} \sum_{t=1}^T (r_i(t) - r_i(t_{ref}))^2}$$
(1)

where In RMSD equation, N is the number of chosen atoms, t_{ref} is correspond to reference time and generally set to 0 for first frame, r_i is the position of the selected atoms belong to the frame x recorded at time t_x . To calculated RMSD this procedure is repeated for every frame along the simulation trajectory. In RMSF equation, t is termed as trajectory time over which RMSF is calculated, reference time is denoted by t_{ref} , r_i is position of residue I, and angular bracket denotes the average over the selection of atoms in the residue. The MD trajectories were analyzed using GROMACS tools and visualized using PyMOL^[36] and VMD^[45]. The ligand-protein interactions and the conformational changes of the protein-ligand complex over the simulation time were analyzed and compared between the different cannabinoid compounds.

3 Results and discussion

3.1 Docking Analysis

The molecular docking of all eight cannabinoid drugs with the 3E9S and 2YDO receptors has been performed. Several cannabinoid compounds exhibited favorable binding affinities to the SARS-CoV-2 RBD, suggesting their potential as inhibitors of the virus. The binding energies of the top-performing cannabinoid compounds, such as Cannabicitrin and Cannabisin D, are -9.11 to -8.84 kcal/mol, respectively, indicating strong and favorable binding affinity. These two compounds also demonstrate a stronger binding affinity with the cannabinoid type 2 receptor, with binding energies of -10.26 and -11.22 kcal/mol. Our results for all ligands with 3E9S and 2YDO proteins show a similar binding trend. If a ligand displays a weaker interaction with 2YDO, it also exhibits a weaker interaction with 3E9S, and vice versa. The binding modes analysis revealed that both Cannabicitrin and Cannabisin D compounds interact efficiently with the 3E9S and 2YDO with multiple interacting site with in the binding pocket. In Figure 4(a,b), the ligand Cannabicitrin shows hydrophobic interaction with the residues 62PRO, 68ARG, 71ALA, and 82PHE inside the binding pocket of 3E9S. Whereas the residues 77THR and 83LEU displays the H-bonding with the ligand. The residue π -Cation Interactions was found between 68ARG and the

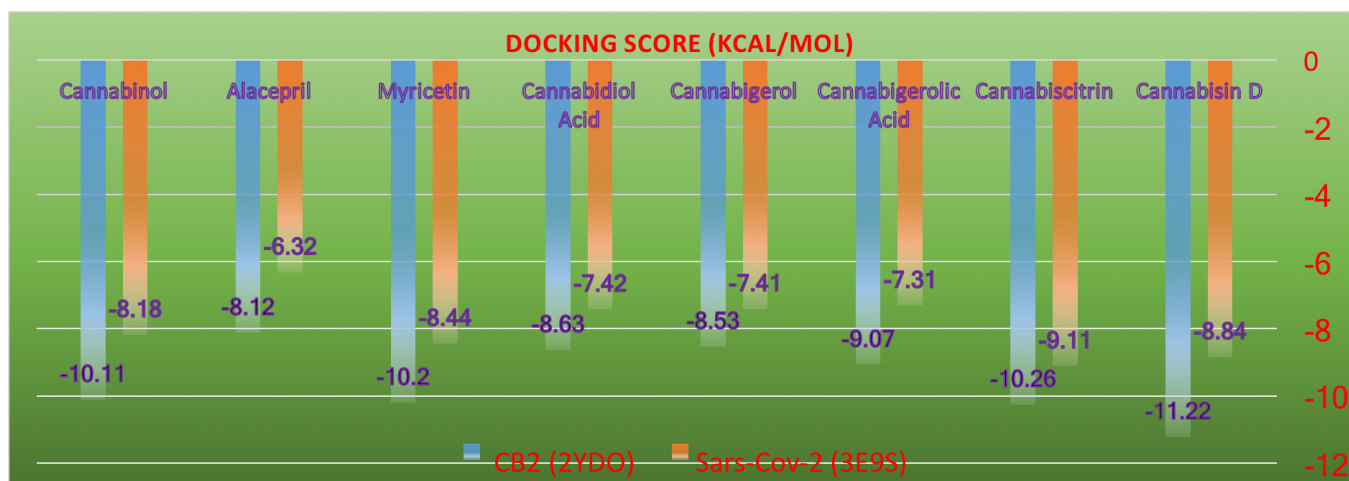


Fig. 3 Docking score for all eight ligands with both proteins

97 Cannabiscitrin ligand. For the case of Cannabisin D as shown in Figure 4(c,d), the residues 249PRO, 250PRO, 266TYR, 270TYR,
 98 271GLN, and 275TYR grabs the ligand by hydrophobic interaction. The ligand also gets stabilized inside the binding pocket with direct
 99 hydrogen bonding with 164LEU, 169GLU, and 270TYR. This Cannabisin D ligand also shows π -Cation Interactions with the 168ARG
 100 residue of 3E9S protein. Similar binding mode analysis has been performed to elucidate the behavior of Cannabiscitrin and Cannabisin
 101 D inside the binding site of the cannabinoid type 2 receptor (See Figure SI2). It was found that the Cannabiscitrin shows hydrophobic
 102 interactions mainly with 168PHE, 246TRP, 249LEU, and 274ILE residues of the target protein. The ligand also shows H-bond interaction
 103 with 66ILE, 169GLU, and 253ASN whereas the 168PHE displays the $\pi - \pi$ interaction with the Cannabiscitrin ligand. Similarly, for the
 104 case of Cannabisin D inside the binding pocket, the residues 66ILE, 84VAL, 167LEU, 168PHE, 169GLU, 249LEU, 267LEU, and 274ILE
 105 shows hydrophobic interaction with docked ligand. The ligand also makes six H-bond with 150LYS, 153LYS, 168PHE, 169GLU, 253ASN,
 106 and 278HIS residues of the receptors which plays a vital role in stabilizing the ligand inside the binding pocket of 2YDO. Apart from
 107 this, the ligand also shows $\pi - \pi$ interaction with the 168PHE residue of target protein (See Figure SI2). We performed the similar
 108 analysis for all the ligand used in the present study and the details of the interaction with both the proteins are presented in SI (See
 109 Ligand Interaction Diagrams and Table for residue details). Overall, these results suggest that Cannabiscitrin and Cannabisin D have
 110 the potential to be inhibitors of the SARS-CoV-2 virus by binding to the RBD of the virus, and further studies are needed to validate
 111 these findings and evaluate their efficacy as COVID-19 therapeutics.

112 3.2 Dynamical Analysis

113 MD simulations are performed on best-docked Cannabiscitrin ligand with receptors "3E9S," and "2YDO," and the temperature, pressure,
 114 and energy are monitored throughout the 50ns of simulation trajectory (Figure SI 5). It is essential that these quantities should remain
 115 constant throughout the simulations which is the key requirement for the stability of the simulations. It is clearly shown in Figure SI
 116 5 that the simulation is stable and not deviating from the initial structure as all the above-mentioned quantities are fluctuating around
 117 the mean initial value. The energy plotted in this figure is the sum of the both kinetic and potential energy of the system. The energy
 118 is plotted in arbitrary units (a.u.), the temperature in Kelvin (K), and pressure in atm. The results for 3E9S and 2YDO are shown for
 119 50 ns which is stable and good enough to compute the various dynamical properties. We can conclude from the Figure that, when the
 120 temperature is on the higher side then the energy of the system also shoots towards the larger values and vice-versa.

121 RMSD (Root Mean Square Deviation) analysis is a widely used method to measure the structural similarity between two protein struc-
 122 tures. It quantifies the average displacement between corresponding atoms in two protein conformations or between a reference
 123 structure and a set of structures. The RMSD for ligand inside the protein 2YDO as represented by black line demonstrates that after
 124 some initial conformational change (adjustment of ligand in the presence of water) becomes stable and remains at the same comfort
 125 zone throughout the simulations. For the cases of 3E9S protein-ligand systems, there is also small fluctuation in RMSD as the ligands
 126 in the 3E9S is more exposed to surrounding water compared to 2YDO where the ligands are sitting well inside the binding pocket of
 127 protein as shown in figure 5a. We conclude from this RMSD result that all the ligands get stable after some initial conformation change
 128 and remain near the binding site throughout the course of simulations as predicted from the molecular docking.

129 An area of the structure with high RMSF (Figure 5b) values frequently diverges from the average, indicating high mobility. When
 130 RMSF analysis is carried out on proteins, it is typically restricted to backbone or alpha-carbon atoms; these are more characteristic of
 131 conformational changes than the more flexible side chains. The RMSF for the C α atoms during MD simulation for all the proteins 3E9S,
 132 and 2YDO are shown in Figure 5 along with RMSD plot.

133 A hydrogen bond is formed by the interaction of a hydrogen atom that is covalently bonded to an electro-negative atom (donor) with

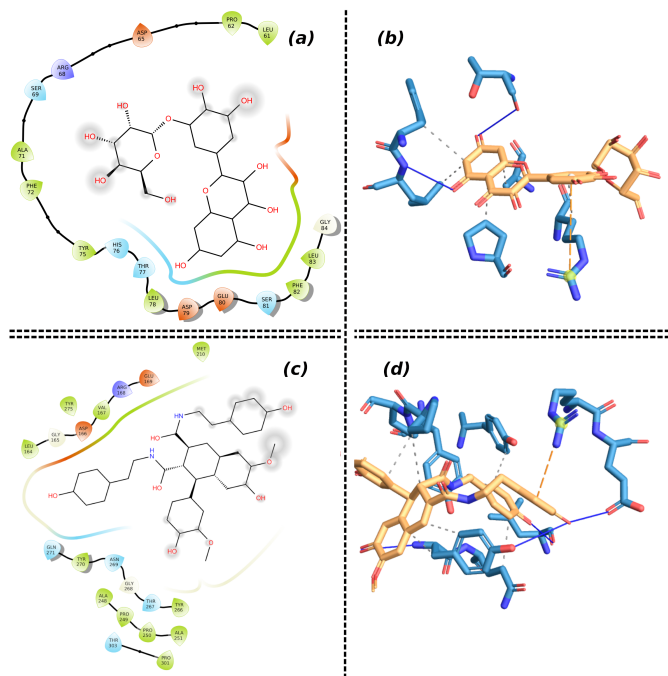


Fig. 4 (a),(c) are 2D Ligand interaction diagram and (b),(d) are 3D Protein ligand interaction of Cannabicitrin and Cannabisisin D with 3E9S, respectively.

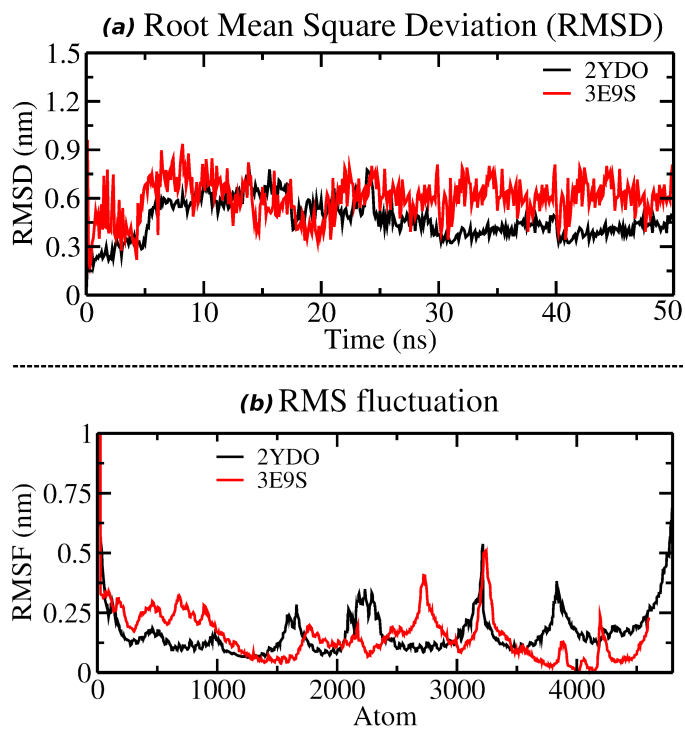


Fig. 5 (a) RMSD values of Ca atoms of native structures of both the proteins. y-axis is RMSD (nm), and the x-axis is time (ns) (b) RMSF values of the carbon alpha over the entire simulation. y-axis is RMSF (nm), and the x-axis is residue.

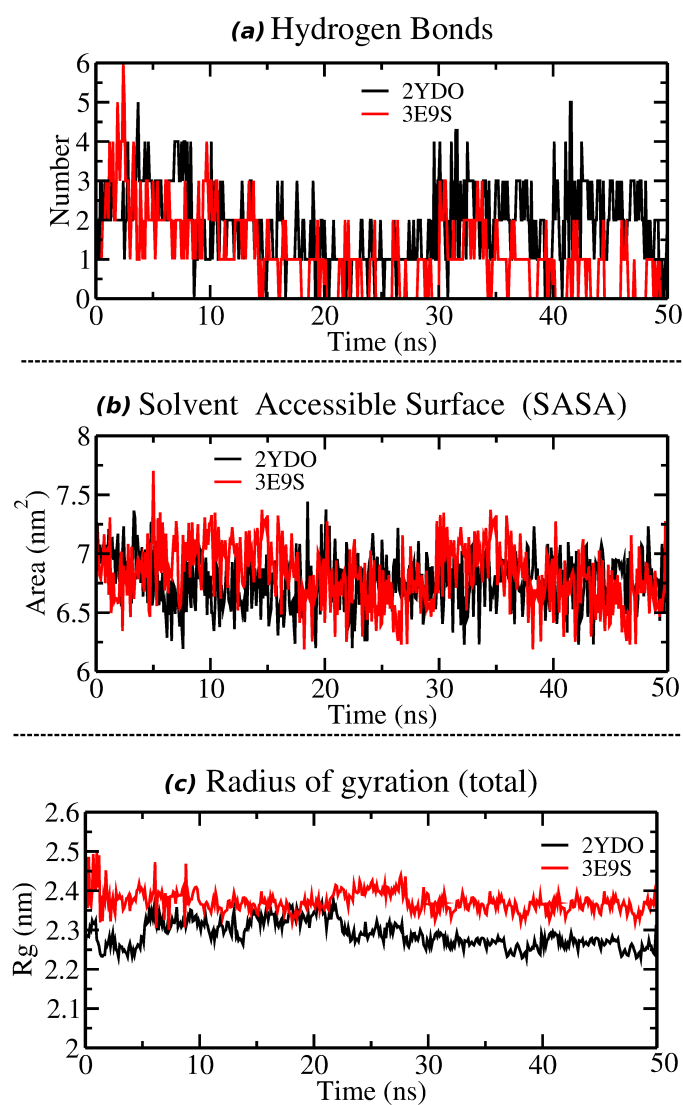


Fig. 6 (a) Total number of H-bond count throughout the simulation, (b) Solvent accessibility of native proteins. y-axis is SASA (nm²), and the x-axis is time (ns), and (c) Rg of both the protein backbone over the entire simulation. y-axis is Rg (nm), and the x-axis is time (ps).

134 another electro-negative atom (acceptor). Hydrogen bonding confers rigidity to the protein structure and specificity to intermolecular
 135 interactions. Hydrogen bonds are crucial in molecular interactions, particularly in biological systems, as they play a significant role in
 136 stabilizing protein structures. We analyze the hydrogen bonds (H-bonds) between all possible donors (D) and acceptors (A) using the
 137 gmxbond program of GROMACS. To determine, if an H-bond exists, a geometrical criterion of $r \leq r_{HB} = 0.35$ nm and an angle cut
 138 off of 30° is used. The receptors 3E9S, and 2YDO exhibit a consistent range of hydrogen bonds between 0 to 3 throughout the entire
 139 simulation. It is clear from the simulation that the ligand-protein docked structure shows stability during the course of simulation by
 140 retaining the similar number of hydrogen bonds with minor fluctuation.

141 Solvent-accessible surface area (SASA) is another crucial property that provides information about the overall protein conformation
 142 in an aqueous environment. Proteins consist of hydrophobic and hydrophilic residues and tend to adopt structures that minimize the
 143 exposure of hydrophobic residues to the aqueous solvent. Increases in SASA from a stable state can indicate protein instability, such as
 144 unfolding that exposes hydrophobic residues to the solvent, leading to undesirable changes like irreversible aggregation. The substitu-
 145 tion of amino acids, whether through mutational or chemical means, can also disrupt the native conformation of a protein, resulting in
 146 partial unfolding and leading to increases in SASA. The SASA value between for our work are ranges between 6.5-10.5 nm² as shown
 147 in Figure 6 explains that the binding of ligands does not affect the folding of the proteins.

148 Radius of gyration was determined to determine the system's compactness over time. Higher Rg values indicate less compactness (more
 149 unfolded) and conformational entropy, whereas low Rg values indicate excellent compactness and structure stability (more folded). The
 150 radius of the gyration plot for both docked proteins after running molecular dynamics simulation were shown in Figure 6. The proteins
 151 3E9S, and 2YDO in the complex were stable, with fewer fluctuations in the Rg value ranging from 2.2-2.5 nm, indicating less variation.

152 The radius of gyration results revealed that the binding of these molecules does not induce structural changes. The plots also show
153 the least fluctuation for 2YDO compared to 3E9S. Overall, these results suggest that Cannabicitrin can form stable complexes with the
154 SARS-CoV-2 RBD and induce conformational changes that lead to a reduction in the distance between key amino acid residues involved
155 in the binding site.
156

157 **4 Conclusions**

158 The objective of this study was to identify antiviral cannabinoid type 2 drugs capable of targeting the main protease (Mpro) of SARS-
159 CoV-2. We utilized standard molecular modeling techniques, including molecular docking and molecular dynamics studies. Cannabis
160 sativa is considered one of the most controversial plants in our society; however, at the same time, it has been used worldwide for
161 medicinal purposes for centuries. In this study, we explored the effects of antiviral cannabinoid type-2 drugs on the recent SARS-COV-2
162 pandemic. We found that Cannabicitrin is the best-suited lead drug candidate against the nucleoprotein (PDB ID: 3E9S) of Covid-19.
163 This protein is a viral protein. Furthermore, through a comparative study, we found that this drug is the most suitable candidate among
164 other existing lead candidates such as Cannabisin D, Cannabinol, Myricetin, etc. We identified the best molecular docking parameter
165 with a binding affinity value of -9.11, which is higher than that of other leading candidates. The therapeutic potential of Cannabicitrin
166 as an antiviral agent has been more critical in combating COVID-19, caused by the severe acute respiratory syndrome corona-virus-2.
167 Based on a computational study, we concluded that the Cannabicitrin drug can better combat the SARS-COV-2 nucleoprotein.

168 **5 Keywords**

169 Docking, antiviral cannabinoid drugs; Sars-CoV-2; Molecular Dynamics.

170 **6 Supplementary Information**

171 See the supplementary material for details on the Cannabinoid Type-2 receptor, ligand interaction diagrams, and a table containing
172 both the residues of the protein and their ligands.

173 **7 Acknowledgments**

174 VKY sincerely acknowledges the University of Allahabad for providing the infrastructure. VKY also thanks Professor Michael L. Klein of
175 Temple University, Philadelphia, USA, for his valuable discussions in setting up the research problem.

176 **8 Author Contributions**

177 MD and VKY performed calculations, analyzed the results and wrote the manuscript.

178 **9 Funding**

179 This research did not receive any specific funding.

180 **10 Data availability**

181 No dataset were generated or analysed during the current study.

182 **11 Conflicts of Interest**

183 The authors declare no conflicts of interest.

184 **References**

- 185 1 World Health Organization. WHO Coronavirus disease (COVID-19) dashboard. Retrieved June 22, 2020, from
186 <https://covid19.who.int/>.
- 187 2 Chen, Y. W., Yiu, C. B., and Wong, K. Y., Prediction of the SARS-CoV-2 (2019-nCoV) 3C-like protease (3CL pro) struc-
188 ture: Virtual screening reveals velpatasvir, ledipasvir, and other drug repurposing candidates. *F1000Research*, 2020, 9, 129.
189 <https://doi.org/10.12688/f1000research.22457.2>
- 190 3 Chen, Y., Liu, Q., and Guo, D., Emerging coronaviruses: Genome structure, replication, and pathogenesis. *Journal of Medical*
191 *Virology*, 2020, **92**(4), 418–423.
- 192 4 Adhikari, S. P., Meng, S., Wu, Y. J., Mao, Y. P., Ye, R. X., Wang, Q. Z., Sun, C., Sylvia, S., Rozelle, S., Raat, H., and Zhou, H.,
193 Epidemiology, causes, clinical manifestation and diagnosis, prevention and control of coronavirus disease (COVID-19) during the
194 early outbreak period: A scoping review. *Infectious Diseases of Poverty*, 2020, **9**(1), 29.
- 195 5 S. R. Weiss, J. L. Leibowitz, Coronavirus pathogenesis. *Adv. Virus Res.* 2021, **81**, 85–164.
- 196 6 Sohrabi, C., Alsafi, Z., O'Neill, N., Khan, M., Kerwan, A., Al-Jabir, A., Iosifidis, C., and Agha, R., World Health Organization declares
197 global emergency: A review of the 2019 novel coronavirus (COVID-19). *International Journal of Surgery (London, England)*, 2020,
198 **76**, 71–76.

- 199 7 Chen, Y. W., Yiu, C. B., and Wong, K. Y., World Health Organization. (2020a). Naming the coronavirus disease (COVID-19) and the
200 virus, 2020,
- 201 8 World Health Organization. (2023). <https://covid19.who.int/>
- 202 9 S. E. Galloway, P. Paul, D. R. MacCannell, M. A. Johansson, J. T. Brooks, A. M. Neil, R. B. Slayton, S. Tong, B. J. Silk, G. L.
203 Armstrong, M. Biggerstaff, V. G. Dugan, Emergence of SARS-CoV-2 B.1.1.7 lineage - United States, December 29, 2020-January 12,
204 2021. *MMWR Morb. Mortal. Wkly Rep.* 2021, **70**, 95–99.
- 205 10 N Zhu, D. Zhang, W. Wang, X. Li, B. Yang, J. Song, X. Zhao, B. Huang, W. Shi, R. Lu, P. Niu, F. Zhan, X. Ma, D. Wang, W. Xu, G. Wu,
206 G.F. Gao, and W. Tan, A novel coronavirus from patients with pneumonia in China, 2019. *New England Journal of Medicine*, 2020,
207 **382(8)**, 727-733.
- 208 11 Geo, Y. R., Cao, Q. D., Hong, Z. S., Tan, Y. Y., Chen, S. D., Jin, H. J., Tan, K. S., Wang, D. Y., and Yan, Y. The origin, transmission and
209 clinical therapies on coronavirus disease 2019 (COVID-19) outbreak - an update on the status. *Military Medical Research*, 2020,
210 **7(1)**, 11. <https://doi.org/10.1186/s40779-020-00240-0>
- 211 12 Di Marzo, V., and Piscitelli, F., The endocannabinoid system and its modulation by phytocannabinoids. *Neurotherapeutics*, 2015,
212 **12(4)**, 692-698.
- 213 13 Klein, T. W., Cannabinoid-based drugs as anti-inflammatory therapeutics. *Nature Reviews Immunology*, 2005, **5(5)**, 400-411.
- 214 14 Ederly, H., Grunfeld, Y., Ben-Zvi, Z. and Mechoulam, R., Structural requirements for cannabinoid activity. *Ann. N.Y. Acad. Sci.*, 1971,
215 **191**, 40–53.
- 216 15 Gaoni, Y. and Mechoulam, R., Isolation, structure and partial synthesis of an active constituent of hashish. *J. Am. Chem. Soc.*, 1964,
217 **86**, 1646–1647
- 218 16 Yadav, V.K., Computational insights into the agonist activity of Cannabinoid receptor type-2 ligands using molecular dynamics
219 simulation. *Current Science*, 2022, **122**, 167–177.
- 220 17 Breemen, R.B.V., Muchiri, R.N., Bates, T.A., Weinstein, J.B., Leier, H.C., Farley, S., and Tafesse, F.G., Cannabinoids Block Cellular
221 Entry of SARS-CoV-2 and the Emerging Variants. *J. Nat. Prod.* 2022, **85**, 176-184.
- 222 18 Martin, B. R., Balster, R. L., Razdan, R. K., Harris, L. S. and Dewey, W. L., Behavioral comparisons of the stereoisomers of tetra-
223 hydrocannabinols. *Life Sci.*, 1981, **29**, 565–574.
- 224 19 Lambert, D. M. and Fowler, C. J., The endocannabinoid system: drug targets, lead compounds and potential therapeutic applications.
225 *J. Med. Chem.*, 2005, **48(16)**, 5059–5087.
- 226 20 Pertwee, R. G., The diverse CB1 and CB2 receptor pharmacology of three plant cannabinoids: delta9-tetrahydrocannabinol,
227 cannabidiol and delta9-tetrahydrocannabivarin. *British Journal of Pharmacology*, 2008, **153(2)**, 199-215.
- 228 21 Chen, C.; Liang, H.; Deng, Y.; Yang, X.; Li, X.; Hou, C. Analysis and Identification of Bioactive Compounds of Cannabinoids in Silico
229 for Inhibition of SARS-CoV-2 and SARS-CoV. *Biomolecules* 2022, **12**, 1729.
- 230 22 Pereira CF, Vargas D, Toneloto FL, Ito VD, Volpato RJ. Implications of Cannabis and Cannabinoid Use in COVID-19: Scoping Review.
231 *Rev Bras Enferm.* 2022;75(Suppl 1):e20201374. <https://doi.org/10.1590/0034-7167-2020-1374>
- 232 23 Paland N, Pechkovsky A, Aswad M, Hamza H, Popov T, Shahar E and Louria-Hayon I., The Immunopathology of COVID-19 and the
233 Cannabis Paradigm. *Front. Immunol.* 2021, **12**, 631233. doi: 10.3389/fimmu.2021.631233
- 234 24 Perez, R.; Glaser, T.; Villegas, C.; Burgos, V.; Ulrich, H.; Paz, C. Therapeutic Effects of Cannabinoids and Their Applications in
235 COVID-19 Treatment. *Life* 2022, **12**, 2117. <https://doi.org/10.3390/life12122117>
- 236 25 Nguyen L.C., Yang,D., Nicolaescu, V., Best,T.J., Gula,H., Saxena,D., Gabbard, J.D., Chen,SN., Ohtsuki,T., Friesen,J.B., Drayma,N.,
237 Mohamed,A., Dann, C., Silva, D., Robinson-Mailman, L., Valdespino, A., Stock, L., Suarez, E., Jones, K.A., Azizi,SA, Demarco,J.K.,
238 Severson, W.E., Anderson, C.D., Millis,J.M., Dickinson, B.C., Tay, S., Oakes, S.A., Pauli,G.F., Palmer, K.E., Meltzer, D.O., Randall,
239 G., and Rosner, M.R., Cannabidiol inhibits SARS-CoV-2 replication through induction of the host ER stress and innate immune
240 responses. *Sci Adv.*, 2022, **8**, eabi6110, doi: 10.1126/sciadv.abi6110.
- 241 26 Olah A., Markovics, A., Szabo-Papp, J., Szabo, P.T., Stott, C., Zouboulis, C.C, and Biro, T., Differential effectiveness of selected
242 non-psychotropic phytocannabinoids on human sebocyte functions implicates their introduction in dry/seborrhoeic skin and acne
243 treatment. *Experimental Dermatology*, 2016, **25(9)**, 701-707.
- 244 27 Raj, V.S., Mou, H., Smits, S.L., Dekkers, D.H.W., Müller, M.A., Dijkman, R., Muth, D., Demmers, J.A.A., Zaki, A., Fouchier, R.A.M.,
245 Thiel, V., Drosten, C., Rottier, P.J.M., Osterhaus, A.D.E.M., Bosch, B.J., and Haagmans, B.L., Dipeptidyl peptidase 4 is a functional
246 receptor for the emerging human coronavirus-EMC. *Nature*, 2013, **495**, 251-254.
- 247 28 K. M. Nelson, J. Bisson, G. Singh, J. G. Graham, S. N. Chen, J. B. Friesen, J. L. Dahlin, M. Niemitz, M. A. Walters, G. F. Pauli, The
248 essential medicinal chemistry of cannabidiol (CBD). *J. Med. Chem.* 2020, **63**, 12137–12155.
- 249 29 H. I. Lowe, N. J. Toyang, W. McLaughlin, Potential of cannabidiol for the treatment of viral hepatitis. *Pharm. Res.*, 2017, **9**, 116–118.
- 250 30 Mahmud, M.S.; Hossain, M.S.; Ahmed, A.T.M.F.; Islam, M.Z.; Sarker, M.E.; Islam, M.R. Antimicrobial and Antiviral (SARS-
251 CoV-2) Potential of Cannabinoids and Cannabis sativa: A Comprehensive Review. *Molecules* 2021, **26**, 7216. <https://doi.org/10.3390/molecules26237216>
- 252

- 253 31 RECOVERY. No Clinical Benefit From Use of Lopinavir-Ritonavir in Hospitalised COVID-19 Patients Studied in RECOVERY. (2020).
254 Available online at: [https://www.recoverytrial.net/news/no-clinical-benefit-from-
255 use-of-lopinavir-ritonavir-in-hospitalised-covid-19-patients-studied-in-recovery](https://www.recoverytrial.net/news/no-clinical-benefit-from-use-of-lopinavir-ritonavir-in-hospitalised-covid-19-patients-studied-in-recovery) (accessed September 14, 2020).
- 256 32 Emberson, J.R., Wiselka, M., Ustianowski, A., Elmahi, E., Prudon, B., Whitehouse, T., Felton, T., Williams, J., Faccenda, J., Under-
257 wood, J., Baillie, J.K., Chappell, L.C., Faust, S.N., Jaki, T., Jeffery, K., Lim, W.S., Montgomery, A., Rowan, K., Tarning, J., Watson,
258 J.A., White, N.J., Juszczak, E., Haynes, R., and Landray, M.J., Effect of hydroxychloroquine in hospitalized patients with Covid-19.
259 *N Engl J Med.* (2020) **383:203**, 1–40. doi: 10.1056/NEJMoa2022926
- 260 33 Agarwal A, Mukherjee A, Kumar G, Chatterjee P, Bhatnagar T, Malhotra P. Convalescent plasma in the management of moderate
261 covid-19 in adults in India: open label phase II multicentre randomised controlled trial (PLACID Trial). *Br Med J.*, 2020, **371**, 3939.
262 doi: 10.1136/bmj.m3939
- 263 34 Paland, N., Pechkovsky, A., Aswad, M., Hamza, H., Popov, T., and Shahar, E. (2021). The Immunopathology of COVID-19 and the
264 Cannabis Paradigm. *Front Immunol.* 2021, **12**, 631233.
- 265 35 <https://www.rcsb.org/>.
- 266 36 <https://pymol.org/2>.
- 267 37 Morris G.M., Huey R., Lindstrom W., Sanner M.F., Belew R.K., Goodsell D.S., Olson A.J. AutoDock4 and AutoDockTools4: automated
268 docking with selective receptor flexibility. *J. Comput. Chem.* 2009, **30**, 2785–2791.
- 269 38 John J. Irwin and Brian K. Shoichet, ZINC – A Free Database of Commercially Available Compounds for Virtual Screening. *J Chem
270 Inf Model*, 2005, **45**, 177–182.
- 271 39 Trott O., Olson A.J. AutoDock Vina: improving the speed and accuracy of docking with a new scoring function, efficient optimization,
272 and multithreading. *J. Comput. Chem.* 2010, **31**, 455–461. doi: 10.1002/jcc.21334.
- 273 40 Van Der Spoel D., Lindahl E., Hess B., Groenhof G., Mark A.E., Berendsen H.J.C. GROMACS: fast, flexible, and free. *J. Comput.
274 Chem.* 2005;26:1701–1718. doi: 10.1002/jcc.20291.
- 275 41 Par Bjelkmar, Per Larsson, Michel A. Cuende, Berk Hess, and Erik Lindahl, Implementation of the CHARMM Force Field in GRO-
276 MACS: Analysis of Protein Stability Effects from Correction Maps, Virtual Interaction Sites, and Water. *Chem. Theory Comput.*,
277 2010, **6(2)**, 459–466.
- 278 42 S. Nose, A molecular dynamics method for simulations in the canonical ensemble, *Mol. Phys.*, 1984, **52**, 255–268.
- 279 43 W.G. Hoover, Canonical dynamics: Equilibrium phase-space distributions, *Phys. Rev. A*, 1985, **31**, 1695–1697.
- 280 44 M. Parrinello and A. Rahman, “Polymorphic transitions in single crystals: A new molecular dynamics method,” *J. Appl. Phys.*, 1981,
281 **52**, 7182–7190.
- 282 45 Humphrey, W., Dalke, A. and Schulten, K., VMD - Visual Molecular Dynamics, *J. Molec. Graphics*, 1996, **14**, 33-38.